Orbital and magnetic ordering in $Pr_{1-x}Ca_xMnO_3$ and $Nd_{1-x}Sr_xMnO_3$ manganites near half doping studied by resonant soft x-ray powder diffraction

U. Staub,[1] M. García-Fernández,[1] Y. Bodenthin,[1] V. Scagnoli,[2] R. A. De Souza,[1] M. Garganourakis,[1] E. Pomjakushina,[3,4] and K. Conder[3]

[1]*Swiss Light Source, Paul Scherrer Institut, 5232 Villigen PSI, Switzerland*

[2]*European Synchrotron Radiation Facility, Boîte Postale 220, 38043 Grenoble Cedex 9, France*

[3]*Laboratory for Developments and Methods, Paul Scherrer Institut, 5232 Villigen PSI, Switzerland*

[4]*Laboratory for Neutron Scattering, PSI & ETH Zürich, 5232 Villigen PSI, Switzerland*

(Received 1 December 2008; revised manuscript received 13 May 2009; published 17 June 2009)

Here we present resonant soft x-ray diffraction data in the vicinity of the Mn $L_{2,3}$ edges on $R_{1-x}T_xMnO_3$ manganites (R=Pr, Nd and T=Ca, Sr) close to half doping. For $Pr_{0.6}Ca_{0.4}MnO_3$ (PCMO), the energy dependence of the superimposed orbital and magnetic reflections are studied using various incident x-ray polarizations. For $Nd_{0.5}Sr_{0.5}MnO_3$ (NSMO), the energy dependence of the orbital ordering reflection is found to be very similar to that found in other manganites systems. These two results are compared to those presented in the literature on single-crystal samples. Whereas our results are in good agreement with the spectral shape of a superposition of magnetic and orbital signals in PCMO, the magnetic signals are only moderately larger than the orbital signals. The results on NSMO do not agree with previously presented data on single crystals and cast doubt on the proposed occurrence of a double-stripe orbital order.

DOI: 10.1103/PhysRevB.79.224419 PACS number(s): 71.30.+h, 75.25.+z, 75.47.Lx, 71.20.Be

I. INTRODUCTION

During the last years doped manganites have attracted considerable attention since they show a variety of electronic and magnetic ground states. The complex phase diagrams as a function of doping and temperature span the range from phases with colossal magnetic resistance to charge and orbitally ordered ground states.[1] The rich variety of states exemplifies the strong interactions between the magnetic and electronic degrees of freedom which are coupled to the crystal lattice. At half doping, three-dimensional $R_{1-x}T_xMnO_3$ (R=Pr, Nd and T=Ca, Sr) perovskites are often antiferromagnetic insulators with charge and orbitally ordered ground states.[2] Though it has been found that the simple picture of a full separation into Mn^{3+} and Mn^{4+} ions is too simplified and the effective charge difference is smaller,[3,4] this simplified picture of charge and orbital order is still useful to describe many properties of the materials around half doping. On the other hand, it is very important to understand the electronic states of the Mn subsystem in detail, in particular, in view of the possible occurrence of Zener polarons[5,6] and the observation of other interesting electronic properties such as of a macroscopic polarization.[7]

Recently, resonant x-ray diffraction has been used to study in detail orbital- and-charge order phenomena in oxides,[8–10] particularly in several manganite systems.[4,11,12] The half doped manganites were studied in the *hard x-ray* regime, where it was found that the resonant process, involving virtual transitions from the core 1s to the 4p states of Mn, mainly probe the charge and orbital order indirectly.[13,14] Such nonmagnetic resonant diffraction signals from space-group forbidden reflections are also called anisotropic tensor of susceptibility (ATS) scattering.

Resonant *soft x-ray* diffraction at the Mn $L_{2,3}$ edges directly probe the Mn 3d states due to a transition from the $2p_{1/2}$, $2p_{3/2}$ to the Mn 3d states, for the L_3 and L_2 edges, respectively. The "half doped" materials treated in these studies, are (a) the 3d perovskites $Pr_{0.6}Ca_{0.4}MnO_3$,[15] $Nd_{0.5}Sr_{0.5}MnO_3$,[16] (b) the A-site ordered $SmBaMn_2O_6$,[17] (c) single layer $La_{0.5}Sr_{1.5}MnO_4$,[18–21] and (d) double layer $LaSr_2Mn_2O_7$.[22] The soft x-ray investigations included the measurement of an orbital superlattice reflection as a function of energy at the Mn $L_{2,3}$ edges. The observed energy dependences for the different materials exhibit significant differences as well as some similarities. The energy spectra of the reflections indicate different types of orbital order,[23,24] and differences observed in their temperature dependence indicate different thermal behaviors in $La_{0.5}Sr_{1.5}MnO_4$ of the orbitals on the one hand and the Jahn-Teller distortion on the other.[18]

Here we are concerned with two materials close to half doping, $Pr_{0.6}Ca_{0.4}MnO_3$ (PCMO) and $Nd_{0.5}Sr_{0.5}MnO_3$ (NSMO). For the slightly less than half doped cubic $Pr_{1-x}Ca_xMnO_3$, it is well known that the charge- and orbital-order state is more stable compared to other rare earths[1] and the material remains insulating. Resonant hard x-ray diffraction demonstrated the orbital- and charge-ordered ground state of the material, though resonant diffraction at the K-edge is an indirect method to access the ordering. Resonant soft x-ray diffraction on $Pr_{0.6}Ca_{0.4}MnO_3$ found that the orbital order is more short range than the magnetic order and that there is a shift in spectral weight between the magnetic and orbital reflection by approximately 3 eV.[15] This is particularly interesting since for half doped $La_{0.5}Sr_{1.5}MnO_4$ there is no such shift. The antiferromagnetic phase transition depends on the effective doping and the magnetic structure is canted, noncollinear,[25] leading to an overlap of magnetic and orbital intensities observed in the soft x-ray resonant diffraction experiment. At lower temperatures an additional magnetic spin reorientation transition was reported.[1]

Half doped $Nd_{0.5}Sr_{0.5}MnO_3$ lies closer to the metallic state and therefore is in the regime where phase-separation effects

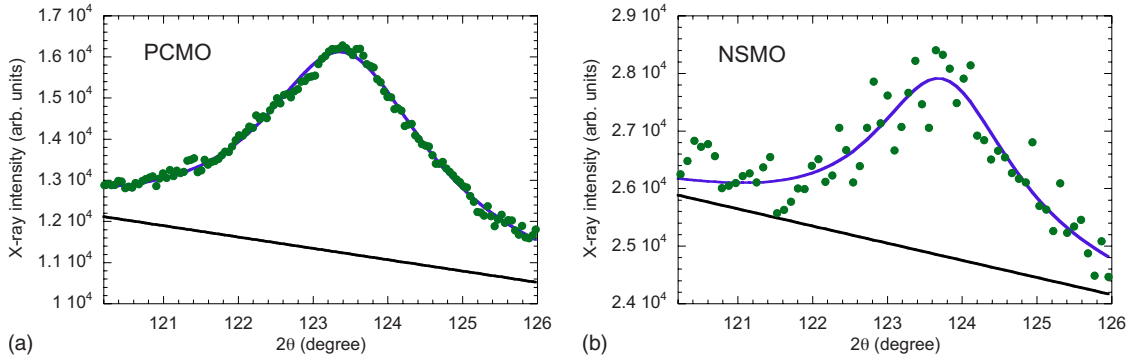

FIG. 1. (Color online) One-dimensional integration of the CCD images, with approximately constant **q**, for the (0 1/2 0) reflections taken with π-incident polarization. Left PCMO $T=25$ K with binning of 10 points, right: NSMO $T=20$ K with binning of 20 points. Data are taken at an x-ray energy of 643 eV.

play a role.[26] A resonant soft x-ray study[16] found that both the (1/2 0 0) and the (0 1/2 0) reflections have an orbital contribution at the Mn $L_{2,3}$ resonances. The analysis of these reflections at resonance was performed in terms of an orbital-bi-striped order model and implied a significant (orbital) charge asphericity occurring at the "Mn^{4+}" sites. Interestingly these two studies also found significantly different energy dependences of the orbital reflection; it would certainly be interesting to clarify these differences as they have important impact on the proposed electronic ground states of the Mn ions.

Here, we show that high-quality resonant soft x-ray diffraction spectra can be obtained on polycrystalline material. We find that the magnetic and orbital signals, which for the PCMO system are superimposed, have similar overall intensities and confirm the 3 eV spectral-weight shift observed previously. For the NSMO system at half doping, we find that the energy dependence is very different compared to that found previously with a single crystal but consistent with that of the orbital signal in PCMO, *A*-site ordered $SmBaMn_2O_6$ and layered $La_{0.5}Sr_{1.5}MnO_4$. This casts serious doubt on the proposed double-stripe model for NSMO.

II. EXPERIMENTS

The samples of $Pr_{0.6}Ca_{0.4}MnO_3$ and $Nd_{0.5}Sr_{0.3}MnO_3$ were synthesized by a solid-state reaction using Pr_6O_{11}, Nd_2O_3, $CaCO_3$, $SrCO_3$, and MnO_2 of a purity exceeding 99.99%. The respective amounts of starting reagents were mixed and calcinated at temperatures of 850–1300 °C during 120 h in air with several intermediate grindings. Phase purity of the synthesized compound was checked by Cu $K\alpha$ x-ray diffraction. Susceptibility was measured with a superconducting quantum interference device (SQUID) and was found to be similar as for these dopings in PCMO and NSMO published in earlier studies. Resonant soft x-ray diffraction experiments were performed on the RESOXS endstation[27] at the surfaces/interfaces microscopy (SIM) beamline of the Swiss Light Source of the Paul Scherrer Institut, Switzerland. A polycrystalline pellet of 10 mm diameter was glued onto a copper sample holder mounted on a He flow cryostat and data was collected between 10 and 300 K. Experiments were performed using linear horizontally or vertically polarized light leading, respectively, to π- and σ-incident photon polarization in the horizontal scattering geometry. Two-dimensional data sets were collected with a commercial Roper Scientific charge-coupled-device (CCD) camera mounted in the ultrahigh vacuum of 1.5×10^{-8} mbar at 300 K. The images were background corrected by subtracting an image taken 5° away from the position in 2θ of the powder ring.

III. RESULTS AND DISCUSSION

A. $Pr_{0.6}Ca_{0.4}MnO_3$

Integrations of the powder diffraction ring of PCMO and NSMO at the Mn L_3 edge are shown in Fig. 1. Since the Bragg angle is of the order of 60° the curvature of the ring is small, and an integration of approximately $\pm2°$ out of the scattering plane, leads to negligible asymmetry in the absorption-limited broadening of the reflections. The integrated intensity of the reflection is obtained by an integration of the image perpendicular to the scattering plane (Fig. 1). A Lorenztian was used to fit the resulting peak. Note that this integration has only a very small effect on the purity of the incoming polarization, σ or π. The energy-dependent integrated x-ray intensities for σ and π incidence and for x-ray fluorescence, collected from the background images, are shown in Fig. 2 for the (1/2 0 0)/(0 1/2 0) reflections. The difference in the *a* and *b* lattice constants is too small to be resolved directly in the experiment and the proposed magnetic (1/2 0 0) and orbital (0 1/2 0) reflections cannot be simply separated. This also applies to the results obtained on the single crystal.[15] However, there the experiment, is performed at given azimuth in contrast to the experiment on the polycrystalline material here, which integrates over all possible azimuthal orientations. The peak with π incidence is larger for almost all energies compared to that with σ incidence at low temperatures. This clearly indicates that there is a significant magnetic contribution because for a magnetic signal, $I_\pi \geq I_\sigma$ due to the absence of a signal in the $\sigma-\sigma$ channel.[28] Moreover, the spectra do not have identical shape, indicative of more than one contribution to the scattering. Notable differences include the shift of the main edge feature of the Mn L_3 edge and the well-resolved peak at 639.8 eV for

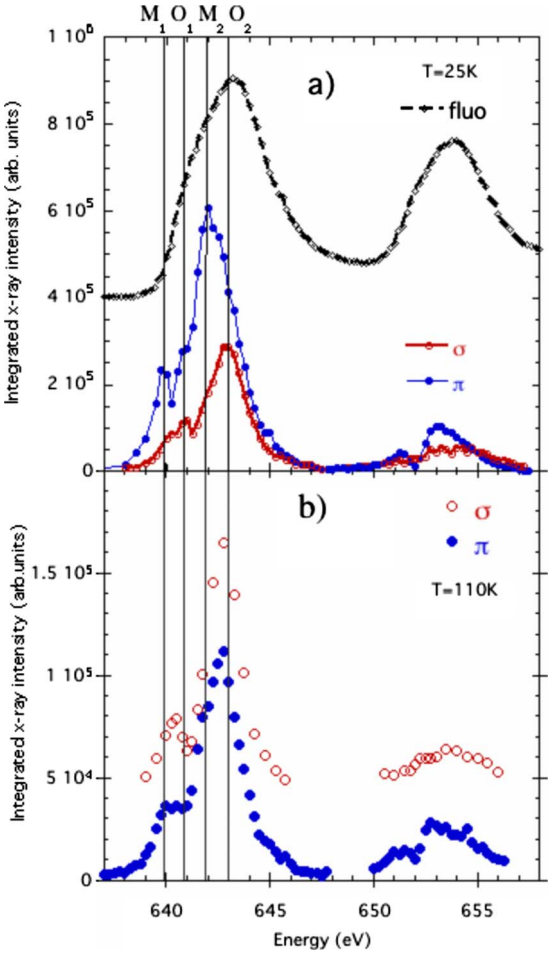

FIG. 2. (Color online) Orbital and magnetic reflections (0 1/2 0)/(1/2 0 0) of $Pr_{0.6}Ca_{0.4}MnO_3$, taken at the Mn $L_{2,3}$ edges at (a) $T=25$ and (b) 110 K with different incoming polarizations (a), lower part; x-ray absorption spectra [fluorescence, (a) upper part]. The vertical lines represent the positions of the magnetic (M) and orbital (O) features at the Mn L_3 edge as compared to the fluorescence data. (b) The spectra are vertically shifted for clarity.

π-incident radiation. A more careful comparison with the spectra collected for the single crystal (Ref. 15) shows few discrepancies with the single-crystal results. Assuming that the intensity of the orbital contribution is the same for σ and π incident [as, e.g., found for $La_{0.5}Sr_{1.5}MnO_4$,[18–21] $Bi_{1-x}Ca_xMnO_3$,[29] and $SmBaMn_2O_6$ (Ref. 17)], the observed spectra at low temperature can roughly be described by a superposition of the spectra assigned to the magnetic and orbital reflections obtained in Ref. 15. Here we label with M_1 and M_2 the main magnetic features observed at the Mn L_3 edge and with O_1 and O_2 the two main orbital features. From such a superposition, one concludes that the orbital reflection intensity is of the same order of magnitude as the magnetic reflection, in strong contrast to the observation on the single crystal, where an orbital signal was almost 2 orders of magnitude weaker.

The feature M_1 appears exactly at the same energy as in Ref. 15, which would support the proposed spectral weight shift between the magnetic and orbital spectra. Figure 2 shows also the same spectra taken at 110 K, still below T_N,

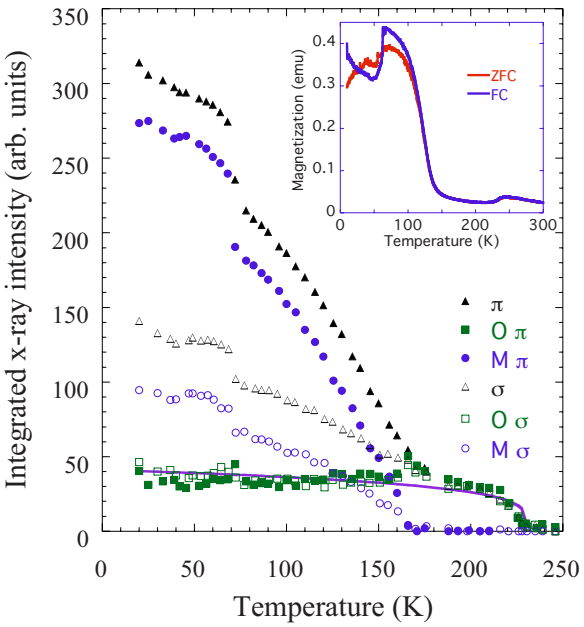

FIG. 3. (Color online) Temperature dependence of the magnetic/orbital reflection of PCMO taken with π- and σ-incident radiation at 643 eV. Also shown are a decomposition of magnetic (M) and orbital (O) contributions by fits as explained in the text. The line is a guide to the eyes for the orbital signals.

where there are clear changes in the spectra compared to 25 K. First there is little shift left between the σ and π main L_3 edge feature. Moreover, at this temperature the lowest-lying spectral feature, M_1, is only weakly visible as a shoulder for the π-incidence data. The spectrum for σ incidence strongly resembles more the orbital signal of the crystal data.[15] In addition, the intensity ratio of the σ- and π-incidence spectra is more close to unity at 110 K, further supporting a dominant orbital signal occurring in the rotated light channel only. The observed difference in intensity between the magnetic and orbital signal, found to be approximately 2 orders of magnitude for the single crystal,[15] might be caused by the particular azimuthal angle chosen. Alternatively, a slight variation of the chemical composition and correspondingly a different canting angle in the magnetic structure, would lead to a different magnetic structure factor. This could lead to a less intense magnetic signal in the (1/2 0 0) magnetic reflection below T_N. Based on such a scenario, we would expect a smaller canting angle in our sample compared to Ref. 15. The differences in the magnetic spectra compared to those from $La_{0.5}Sr_{1.5}MnO_4$,[18,19,24] where there is no spectral-weight difference of 3 eV between magnetic and orbital signal may have the same origin. The different in-plane canting angle of the magnetic moments in the two materials[19,30] may lead to different admixture of magnetic Mn^{3+} and Mn^{4+} moment contributions with individually different energy spectra.

The temperature dependence of the observed signal at resonance is shown in Fig. 3 for both σ- and π-incident polarizations. There are three transitions observed as predicted by the phase diagram of Ca-doped PCMO below half doping. The charge and orbital transition are around 240 K followed by the antiferromagnetic transition at 170 K. At low temperatures, the magnetic reorientation transition is visible

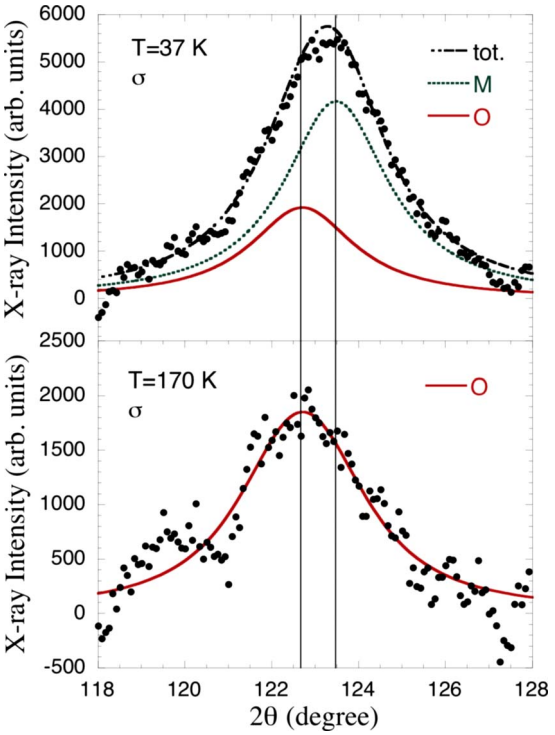

FIG. 4. (Color online) Magnetic and orbital reflections of PCMO taken with σ-incident radiation at 643 eV and different temperatures decomposed of magnetic (M) and orbital (O) Lorentzians. Positions highlighted by vertical lines.

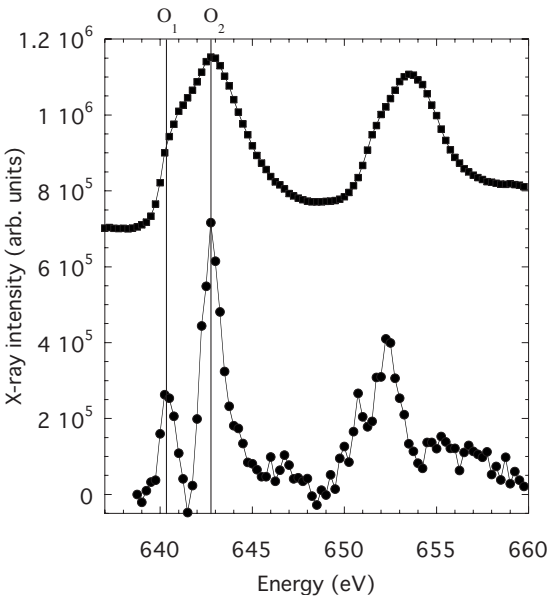

FIG. 5. Energy dependence of the (0 1/2 0) orbital reflection with π-incident radiation in $Nd_{0.5}Sr_{0.5}MnO_3$, taken at 20 K and with π-incident radiation.

at 70 K, with an increase in the canting angle, reflected by an increase in the magnetic intensity. These transitions are also observed in the magnetization as shown in the inset of Fig. 3. Above T_N the intensity of the (0 1/2 0) reflections is equal for σ- and π-incident radiation, indicating that the signal occurs only in the rotated polarization channels. Note that the σ-σ and π-π channels have different intensities as they depend differently on the Bragg angle,[31] and have been shown to be absent in other half doped manganties using polarization analysis of scattered radiation.[19] The high-momentum resolution of soft x-ray diffraction allows us to disentangle the two contributions. At high temperature the position represents the pure orbital (0 1/2 0) and the low-temperature peak is a superposition of the magnetic (1/2 0 0) and orbital (0 1/2 0) reflections (see Fig. 4). Fitting the reflection with two Lorenztians keeping extracted positions fixed of the (1/2 0 0) and (0 1/2 0) reflections results in temperature dependences of the orbital and magnetic contributions as shown in Fig. 3. These results show that even though both reflection d spacings differ very little ($d \approx 0.03$ Å) in agreement with the expected lattice constants determined by structural studies,[32] the individual intensities can be roughly separated. The intensity ratio between magnetic and orbital reflections are 2.5 and 7 for σ- and π-incident polarization, respectively, and are much smaller as previously reported.[15]

B. $Nd_{0.5}Sr_{0.5}MnO_3$ (NSMO)

For the NSMO system, the energy dependence of the (0 1/2 0) reflection is shown in Fig. 5 together with the fluorescence spectra extracted from the background intensities. The expected difference in the a and b lattice constants[16] is approximately 1.15% and the separation in 2θ of (1/2 0 0) and (0 1/2 0) is approximately 2.1°. Both reflection positions are contained in the data window and therefore, the obtained integrated data would reflect at least in part a superposition of the two reflections. However, the experimental data do not give support for the occurrence of the (1/2 0 0) reflection. The energy spectrum is very different compared to the peak maximum intensity of (1/2 0 0), (0 1/2 0) or a superposition of these collected on a single crystal.[16] In the raw spectra of the single-crystal study, the fluorescence signal is contributing significantly to the signal. In contrast, in our powder diffraction experiment we obtain the integrated intensity, which inherently does not contain the fluorescence contribution. Moreover, additional broadenings due the changing penetration depth[33,34] and refraction effects[33,35] are inherently corrected for by the average over the powder grains as its collected data represents q scans. It is also interesting to compare the energy dependence for the orbital reflection with those of other half doped systems such as the previously mentioned $Pr_{0.4}Ca_{0.6}MnO_3$ for $T > T_N$,[15] half doped $SmBaMn_2O_6$ (Ref. 17) and half doped single layer $La_{0.5}Sr_{1.5}MnO_4$:[19–21] they all have quite similar energy dependences. Except for some small distinct differences this spectral shape therefore seems to be representative for half doping. These differences have been used to differentiate[17] between x^2-y^2- and $3r^2$-z^2-type orbital order for $SmBaMn_2O_6$ and $La_{0.5}Sr_{1.5}MnO_4$.[17] To apply such arguments here, however, would require higher-quality data in which the individual weak features can be precisely determined. The overall agreement on the spectral shape imposes a strong constraint on the possible electronic states, the variation of which is expected to be small, despite the different long-range-ordered crystal structure of these materials.

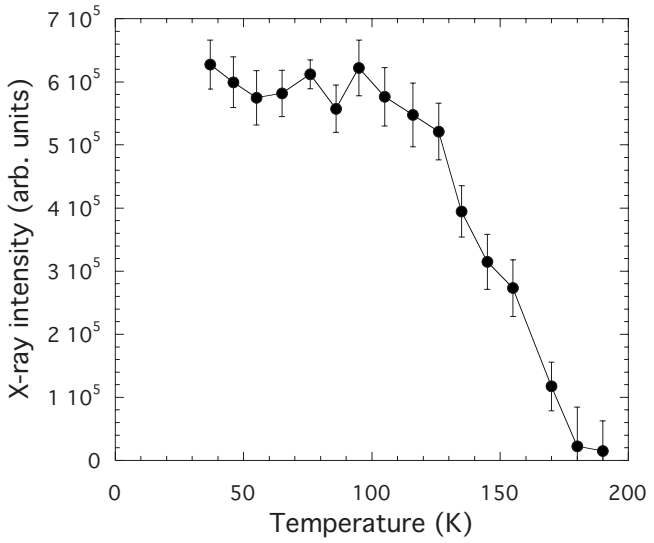

FIG. 6. Temperature dependence of the (0 1/2 0) orbital reflection in $Nd_{0.5}Sr_{0.5}MnO_3$ taken at the Mn L_3 edge with π-incident radiation.

The temperature dependence of the intensity of the main edge feature at 643 eV is shown in Fig. 6. The orbital signal disappears at the orbital-order phase transition at approximately 170 K. The intensity at this energy is the same for π and σ incidence, which indicates that the diffracted intensity is purely in the rotated channel, with no contribution in the unrotated channel. As every point in the spectra represents an average over all the possible azimuthal angles (powder average), this clearly supports the orbital origin or a so-called ATS scattering. This scattering is a measure of the quadrupole of the Mn 3*d* shell caused by the orbital order of the e_g states.

A comparison with the PCMO spectra indicates that the first feature in PCMO indeed occurs at lower energy compared to the NSMO absorption spectra. The spectral difference between the (0 1/2 0) reflection from Ref. 16 could possibly be understood by a stronger absorption correction to the intrinsic energy dependence of the reflection caused by a thin dead layer (not orbitally ordered) at the surface. This would mostly affect the intensity at the main edge feature (643 eV), where the absorption is strongest, and would lead to a relative enhancement of the L_2 edges signal. Such an effect may also be the origin of the differences observed[22] for the $LaSr_2Mn_2O_7$ compared to the other orbital peaks in other manganites. A surface degradation in manganites has already been found in these double layer manganites.[36] The broad peak observed at the L_2 edge in Ref. 16 cannot be solely caused by the fluorescence signal and reflects an unidentified scattering contribution, even for $T=180$ K. In particular, fluorescence is larger at the L_3 edge compared to L_2, which is nicely shown in Figs. 2 and 5. Therefore, the weaker and broad features observed at the (1/2 0 0) reflection in NSMO are not necessary caused by Bragg diffraction. Moreover, we would like to mention that the difference of lattice constants in *a* and *b* of NSMO would only lead to a different 2θ of 2.1°, which is not sufficiently large to completely suppress the second domain. Figures 1(a) and 1(b) show that the intrinsic width of the reflection is large due to the limited penetration depth and we expect an approximately 20% contribution of the (0 1/2 0) reflection at the (1/2 0 0) position. An alternative scenario could be that there is an additional magnetic signal observed in the single-crystal study because our first spectral feature at the L_3 edge lies slightly lower in energy than the O_1 feature. These observations put into question the interpretation of the observation of a resonant (1/2 0 0) reflection and correspondingly on a double-stripe ordering in NSMO.[16]

IV. CONCLUSIONS

Our resonant soft x-ray powder diffraction experiments on $Pr_{0.6}Ca_{0.4}MnO_3$ and $Nd_{0.5}Sr_{0.5}MnO_3$ support orbital order of the Mn 3*d* shell. They clearly support the occurrence of different signals in the PCMO, although the average over the azimuthal angles is inconsistent with the previous results that the magnetic signal is 2 orders of magnitude larger than the orbital. This difference is possibly caused by a different canting angle of the magnetic moments. The results obtained on half doped NSMO are consistent with the simple orbital- and charge-order picture. They show that the orbital-order reflection at half doping has a characteristic energy dependence. This result raises doubts on the data and interpretation of the previous work on single crystals and does not support a double-stripe orbital order. Moreover, our results indicate that resonant soft x-ray diffraction can be easily and successfully performed also on powder materials.

ACKNOWLEDGMENTS

We thank the beamline staff of X11MA for their excellent support and the provision of experimental equipment by J. M. Tonnerre and we thank K. Prsa and S. Weyneth for their assistance in sample characterization. We also thank S. Grenier for stimulating discussions. This work was supported by the Swiss National Science Foundation and the NCCR MaNEP Project and performed at SLS of the Paul Scherrer Insitut, Villigen PSI, Switzerland.

[1] E. Dagotto, T. Hotta, and A. Moreo, Phys. Rep. **344**, 1 (2001).
[2] P. Schiffer, A. P. Ramirez, W. Bao, and S.-W. Cheong, Phys. Rev. Lett. **75**, 3336 (1995).
[3] J. Herrero-Martín, J. García, G. Subias, J. Blasco, and M. Concepción Sanchez, Phys. Rev. B **70**, 024408 (2004).
[4] S. Grenier, J. P. Hill, D. Gibbs, and K. J. Thomas, M. v. Zimmermann, C. S. Nelson, V. Kiryukhin, Y. Tokura, Y. Tomioka, D. Casa, T. Gog, and C. Venkataraman, Phys. Rev. B **69**, 134419 (2004).
[5] D. V. Efremov, J. van den Brink, and D. I. Khomskii, Nature

Mater. **3**, 853 (2004).
[6] A. Daoud-Aladine, J. Rodríguez-Carvajal, L. Pinsard-Gaudart, M. T. Fernández-Díaz, and A. Revcolevschi, Phys. Rev. Lett. **89**, 097205 (2002).
[7] Y. Tokunaga, T. Lottermoser, Y. Lee, R. Kumai, M. Uchida, T. Arima, and Y. Tokura, Nature Mater. **5**, 937 (2006).
[8] Y. Murakami, J. P. Hill, D. Gibbs, M. Blume, I. Koyama, M. Tanaka, H. Kawata, T. Arima, Y. Tokura, K. Hirota, and Y. Endoh, Phys. Rev. Lett. **81**, 582 (1998).
[9] H. Nakao, K. Ohwada, N. Takesue, Y. Fujii, M. Isobe, and Y. Ueda, M. v. Zimmermann, J. P. Hill, D. Gibbs, J. C. Woicik, I. Koyama, and Y. Murakami, Phys. Rev. Lett. **85**, 4349 (2000).
[10] U. Staub, G. I. Meijer, F. Fauth, R. Allenspach, J. G. Bednorz, J. Karpinski, S. M. Kazakov, L. Paolasini, and F. d'Acapito, Phys. Rev. Lett. **88**, 126402 (2002).
[11] Y. Murakami, H. Kawada, H. Kawata, M. Tanaka, T. Arima, Y. Moritomo, and Y. Tokura, Phys. Rev. Lett. **80**, 1932 (1998).
[12] J. Geck, P. Wochner, S. Kiele, R. Klingeler, P. Reutler, A. Revcolevschi, and B. Büchner, Phys. Rev. Lett. **95**, 236401 (2005).
[13] P. Benedetti, J. van den Brink, E. Pavarini, A. Vigliante, and P. Wochner, Phys. Rev. B **63**, 060408(R) (2001).
[14] M. Benfatto, Y. Joly, and C. R. Natoli, Phys. Rev. Lett. **83**, 636 (1999).
[15] K. J. Thomas, J. P. Hill, S. Grenier, Y.-J. Kim, P. Abbamonte, L. Venema, A. Rusydi, Y. Tomioka, Y. Tokura, D. F. McMorrow, G. Sawatzky, and M. van Veenendaal, Phys. Rev. Lett. **92**, 237204 (2004).
[16] J. Herrero-Martín, J. García, G. Subias, J. Blasco, M. Concepción Sanchez, and S. Stanescu, Phys. Rev. B **73**, 224407 (2006).
[17] M. García-Fernández, U. Staub, Y. Bodenthin, S. M. Lawrence, A. M. Mulders, C. E. Buckley, S. Weyeneth, E. Pomjakushina, and K. Conder, Phys. Rev. B **77**, 060402(R) (2008).
[18] U. Staub, V. Scagnoli, A. M. Mulders, M. Janousch, Z. Honda, and J. M. Tonnerre, Europhys. Lett. **76**, 926 (2006).
[19] U. Staub, V. Scagnoli, A. M. Mulders, K. Katsumata, Z. Honda, H. Grimmer, M. Horisberger, and J. M. Tonnerre, Phys. Rev. B **71**, 214421 (2005).
[20] S. S. Dhesi, A. Mirone, C. De Nadai, P. Ohresser, P. Bencok, N. B. Brookes, P. Reutler, A. Revcolevschi, A. Tagliaferri, O. Toulemonde, and G. van der Laan, Phys. Rev. Lett. **92**, 056403 (2004).
[21] S. B. Wilkins, P. D. Spencer, P. D. Hatton, S. P. Collins, M. D. Roper, D. Prabhakaran, and A. T. Boothroyd, Phys. Rev. Lett. **91**, 167205 (2003).
[22] S. Wilkins, N. Stoic, T. A. W. Beale, N. Binggeli, P. D. Hatton, P. Bencok, S. Stanescu, J. F. Mitchell, P. Abbamonte, and M. Altarell, J. Phys.: Condens. Matter **18**, L323 (2006).
[23] A. Mirone, S. S. Dhesi, and G. van der Laan, Eur. Phys. J. B **53**, 23 (2006).
[24] S. B. Wilkins, N. Stojic, T. A. W. Beale, N. Binggeli, C. W. M. Castleton, P. Bencok, D. Prabhakaran, A. T. Boothroyd, P. D. Hatton, and M. Altarelli, Phys. Rev. B **71**, 245102 (2005).
[25] H. Yoshizawa, H. Kawano, Y. Tomioka, and Y. Tokura, Phys. Rev. B **52**, R13145 (1995).
[26] C. Ritter, R. Mahendiran, M. R. Ibarra, L. Morellon, A. Maignan, B. Raveau, and C. N. R. Rao, Phys. Rev. B **61**, R9229 (2000).
[27] U. Staub, V. Scagnoli, Y. Bodenthin, M. García-Fernández, R. Wetter, A. M. Mulders, H. Grimmer, and M. Horisberger, J. Synchroton Radiat. **15**, 469 (2008).
[28] S. W. Lovesey and S. P. Collins, *X-Ray Scattering and Absorption by Magnetic Materials* (Clarendon, Oxford, 1996).
[29] S. Grenier, V. Kiryukhin, S.-W. Cheong, B. G. Kim, J. P. Hill, K. J. Thomas, J. M. Tonnerre, Y. Joly, U. Staub, and V. Scagnoli, Phys. Rev. B **75**, 085101 (2007).
[30] B. J. Sternlieb, J. P. Hill, U. C. Wildgruber, G. M. Luke, B. Nachumi, Y. Moritomo, and Y. Tokura, Phys. Rev. Lett. **76**, 2169 (1996).
[31] S. W. Lovesey, E. Balcar, K. S. Knight, and J. Fernandez-Rodriguez, Phys. Rep. **411**, 233 (2005).
[32] M. R. Lees, J. Barratt, G. Balakrishnan, D. M. Paul, and C. Ritter, Phys. Rev. B **58**, 8694 (1998).
[33] L. Sève, J. M. Tonnerre, and D. Raoux, J. Appl. Crystallogr. **31**, 700 (1998).
[34] U. Staub, O. Zaharko, H. Grimmer, M. Horisberger, and F. d'Acapito, EPL **56**, 241 (2001).
[35] U. Staub, M. Shi, C. Schulze-Briese, B. D. Patterson, F. Fauth, E. Dooryhee, L. Soderholm, J. O. Cross, D. Mannix, and A. Ochiai, Phys. Rev. B **71**, 075115 (2005).
[36] J. W. Freeland, K. E. Gray, L. Ozyuzer, P. Berghuis, E. Badica, J. Kavich, H. Zheng, and J. F. Mitchell, Nature Mater. **4**, 62 (2005).